Surface phonon dispersion in graphite and in a lanthanum graphite intercalation compound

Susanne Siebentritt,* Roland Pues, Karl-Heinz Rieder
Fachbereich Physik, Free University Berlin, Arnimallee 14, 14195 Berlin, Germany

Alexander M. Shikin
Institute of Physics, St. Petersburg State University, St. Petersburg, 198904 Russia
(Received 26 August 1996)

Using high-resolution electron energy-loss spectroscopy the surface-phonon dispersion of graphite has been determined in the ΓK direction over the whole energy range and the whole Brillouin zone. Born–von Karman model calculations are used to describe the dispersion relations. An unexpected result is the splitting of the *ZA* and *ZO* mode at the *K* point. Following a previously introduced procedure to form *in situ* rare-earth graphite intercalation compounds (GIC), which for lanthanum results in an intermediate carbide phase, we prepared this carbidic phase and the final GIC-like phase. The carbide shows five dispersionless features that may be attributed to Einstein modes of graphite islands. The phonon dispersion of the final phase shows the same modes as graphite shifted in energy: softening of the optical and stiffening of the acoustical phonons occurs. This is described within a Born–von Karman model by weakening the nearest-neighbor interaction and strengthening the second-nearest-neighbor interaction. The evolution of the phonon dispersion gives a first hint that the GIC-like phase may develop in two stages: first a monolayer graphene on top of the carbide and then the very thin GIC layer. [S0163-1829(97)06012-8]

I. INTRODUCTION

Recently there has been renewed interest in graphite intercalation compounds (GIC) since a simple *in situ* method has been developed to prepare rare-earth GIC's.[1] This paper is devoted to the investigation by high-resolution electron energy-loss spectroscopy (HREELS) of the surface-phonon dispersion relations of pure graphite in the ΓK direction, of its GIC-like modification with lanthanum, and of an intermediate lanthanum carbide modification.

The phonon dispersion of the graphite (0001) surface over the entire surface Brillouin zone between the Γ and *M* points and the entire energy region was not measured before 1988 when it was obtained by Oshima and co-workers[2] using HREELS. In 1987, Wilkes, Palmer, and Willis published an HREELS study of the surface phonons of graphite as well;[3] this was performed on highly oriented pyrolytic graphite, which is azimuthally disordered. To our knowledge no measurements exist so far in the other high-symmetry direction ΓK. Here we present the determination of the surface-phonon dispersion over the whole energy range and over the whole Brillouin zone in the ΓK direction and show the results of a Born–von Karman model calculation describing the phonon dispersion. Since the existing models for the phonon dispersion in graphite have been fitted along ΓM this provides an excellent check on the parametrization. Due to the layered structure of graphite the surface phonons are basically identical to the bulk phonons.[3]

Initially the interest in the La-graphite system arose from the work on the electronic structure of lanthanum GIC.[1,4–7] There a method has been developed to form *in situ* rare-earth GIC's by vapor deposition of a film of the rare-earth metal, e.g., Eu, Yb, or La, onto the graphite surface followed by thermal annealing. In the case of Eu or Yb this leads to the formation of the corresponding intercalation compound.[8,9] With lanthanum the problem arises that it forms carbides very readily due to its chemically active *d* electrons. In early work on GIC's it has been said that due to carbide formation it is not possible to form La GIC.[10] And indeed upon annealing the La film on top of the graphite at moderate temperatures (1000 K) a thick layer of lanthanum carbide is formed[5] whereas in the case of Eu and Yb a carbide phase is not observed[8,9] at the experimental conditions applied. The surface of the carbidic phase is most likely terminated by La atoms.[6] Here we will present the vibrational spectra of this carbidic phase as well.

Further annealing at higher temperatures (1300 K or more) leads to the accumulation of carbon on the carbide surface which at these temperatures is most likely the (111) surface of the ε modification of LaC_2 (CaF_2 structure).[6] On top of the (La terminated) carbide a very thin (a few Å) graphitic layer is formed. It has not been clear whether this constitutes a monolayer graphene (MLG) on the carbide or a film of GIC just a few monolayers thick.[6,7] The same behavior is observed for other carbides, e.g., SIC, which also forms a graphitic layer upon heating.[11] The geometrical and electronic structure of the graphitic layer on La carbide is very much like that of alkali graphite intercalation compounds[5] with an ordered $(\sqrt{3}\times\sqrt{3})R30°$ superstructure and charge transfer from the metal to the graphite layer. The superstructure is compatible with La intercalated between the graphite layers or with an MLG on the (111) surface of ε-LaC_2, the surface unit cell of which matches the unit cell of $(\sqrt{3}\times\sqrt{3})$ graphene within 0.5%. The transferred charge occupies states in the antibonding π^* bands of the graphite, which shows up as a characteristic peak at 280 eV in the Auger spectra: a moderate peak somewhat higher in energy than the carbon peak.[5]

Monolayers of graphene have been previously investigated on—among other surfaces—transition-metal

carbides.[12–16] These systems also show a GIC-like electronic structure. However, on these surfaces the interaction between the graphene layer and the carbide is not due to charge transfer—as can be seen from the Auger spectra, which do not show the 280-eV peak or only a weak shoulder[13]—but due to covalent bonding between the carbon atoms in the graphene layer and the metal atoms in the carbide.[14,16] Phonon dispersions have been measured for MLG's on a number of transition-metal carbides.[12,13] The first observation is that the modes detected in bulk graphite remain present in the MLG on carbide, indicating that the structure is basically unaltered. But the modes in MLG are lower in energy. This can be modeled by the Born–von Karman model by Aizawa *et al.*[13] containing six coupling constants for bond stretching between nearest and second-nearest neighbors, bond bending, and bond twisting. The softening of the graphite modes in the MLG is described by a weaker coupling for all the interactions.

On the phonon dispersion in GIC's not much information is available for the in-plane wave vectors. It is known that for donor GIC's the optical phonons at the Γ point shift towards lower energies as compared to graphite.[17] In Li-GIC the lowest acoustical mode with in-plane propagation is observed to shift to lower energies as well.[18]

Here we present the phonon dispersion of the GIC-like phase of the La-graphite system in the ΓK direction of the underlying graphite substrate as measured with HREELS and discuss the implication for the question whether it constitutes a very thin GIC layer or an MLG on carbide. We will show that the dispersion relations can be described within the model by Aizawa *et al.* with the appropriate choice of force constants.

II. EXPERIMENT

Our experiments are conducted in a UHV system with background pressure better than 5×10^{-11} mbar equipped with an ELS22 HREEL spectrometer, consisting of two double cylindrical 127° deflectors, a low-energy electron diffraction (LEED) system capable of retarding field Auger electron spectroscopy (AES), and a quadrupole mass spectrometer. The residual gas consists mainly of H_2 with small fractions of H_2O, CO, and CO_2. The evaporator for lanthanum is self-made by welding a small piece of La onto a W-Re wire immediately previous to mounting it into the vacuum chamber. The evaporator is calibrated using a quartz microbalance. The sample holder can be heated resistively up to 1500 K and cooled down to 100 K using liquid nitrogen.

The substrate is a natural flake of graphite with high crystallinity as seen from the clear hexagonal LEED pattern. It is cleaved using adhesive tape in ambient atmosphere and heated in UHV to 1300 K for several hours. The purity is verified by Auger and HREEL spectroscopy.

The GIC-like structure is prepared by depositing a 60–100-Å-thick film onto the graphite at room temperature and a subsequent successive annealing procedure. The system is heated step by step and investigated at each annealing step by LEED, AES, and HREELS at room temperature.

HREELS has been performed at a primary energy of 20 eV and an energy width of the elastic reflected beam of about 8–10 meV. This primary energy has been chosen in order to provide a parallel momentum transfer high enough to reach the Brillouin zone boundary. The incident angle is 60°, 70°, or 75° towards the surface normal, and the detection angle can be varied within the sagittal plane between 75° and 10°, that is a maximal off-specular angle φ of 65° (Fig. 1). Different incident angles are used since the energy losses at low off-specular angles (low parallel momentum transfer) are clearer at steep incidence whereas the losses at high off specular angles are seen better at low angle incidence. The sample is mounted such that the sagittal plane is along the ΓK direction.

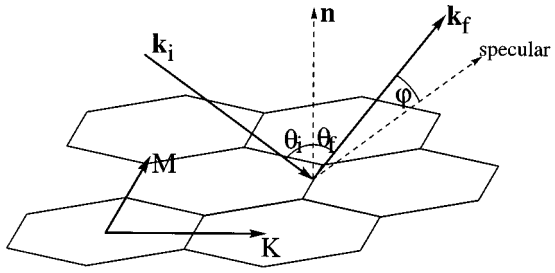

FIG. 1. Scattering geometry. Indicated are the incident angle θ_i, the detection angle θ_f, the scattering angle φ, the incident momentum $\mathbf{k}_i$, and the final momentum $\mathbf{k}_f$.

III. RESULTS AND DISCUSSION

A. Pure graphite: Experimental

Figure 2 shows a series of HREEL spectra taken at different off-specular angles φ, that is, at different parallel momentum transfer $\mathbf{q}_\parallel=\mathbf{k}_{f,\parallel}-\mathbf{k}_{i,\parallel}$. Six different modes can be distinguished: three optical ones and three acoustical ones—as one would expect for a surface with two atoms in the unit cell. From the energy losses at different momentum transfer the surface dispersion relations $\omega(q_\parallel)$ can be derived, which are displayed in Fig. 3. The polarization of the modes is derived from calculations according to the model by Aizawa *et al.* (see below). The different modes are the vertical acoustical mode ZA, the acoustical shear horizontal mode SH, the longitudinal acoustical mode LA, the vertical optical mode ZO, the optical shear horizontal mode SH*, and the longitudinal optical mode LO. According to the HREELS selection rules the shear modes should not be detected and as seen in Fig. 2 the acoustical SH mode has indeed a very low scattering cross section. But since the crystal is a thin flake attached only at the edges some buckling might occur that would lift the selection rules. To our knowledge these are the first measurements of the surface phonons of graphite in ΓK direction over the whole energy region. A number of models and *ab initio* calculations that have been checked against the results in the ΓM direction also predict the phonon dispersion for the ΓK direction: *ab initio* calculations in the local density direct approach,[19] in the local density linear-response approach,[20] and the bond charge model.[21] The direct approach *ab initio* calculations give excellent agreement with our experimental data besides some peculiarities at the K point to be discussed below. Phonon dispersions obtained from the force constant model by Aizawa *et al.*[13] have been

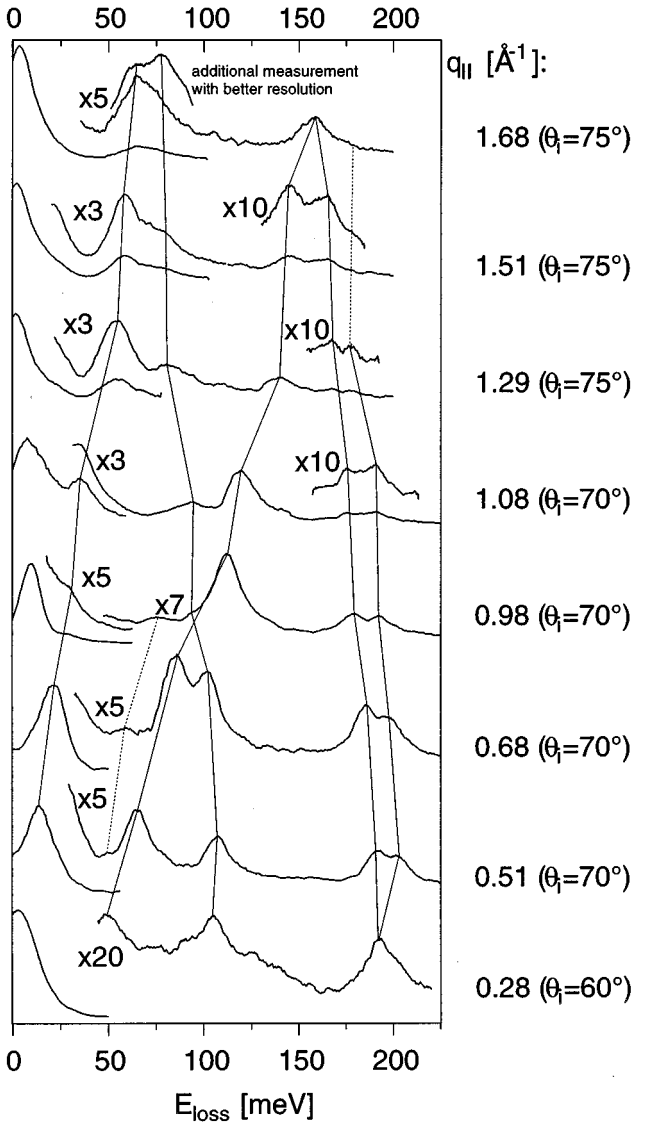

FIG. 2. Series of HREEL spectra on pure graphite at different scattering angles corresponding to increasing parallel momentum transfer. Six modes can be distinguished. Different incident angles were used and are given in brackets.

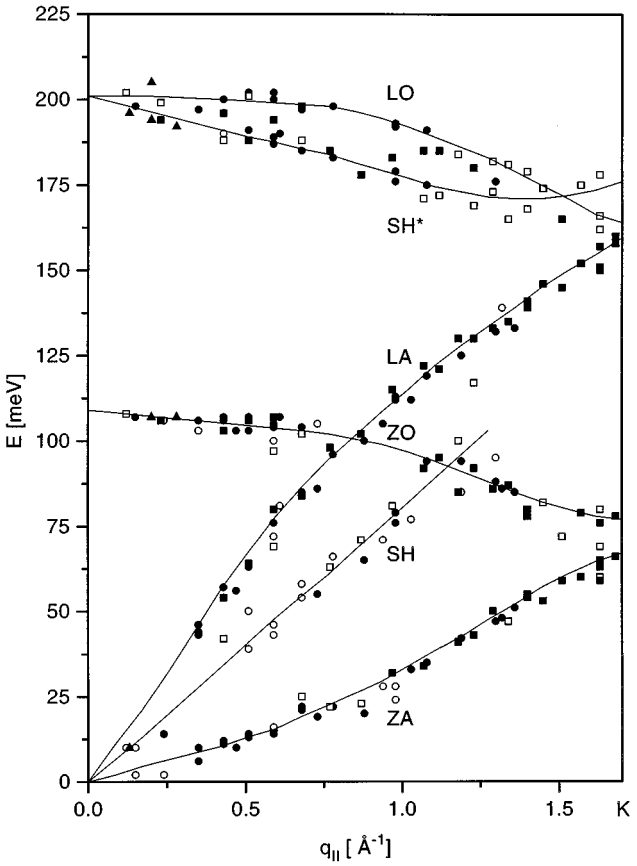

FIG. 3. The experimentally determined dispersion relation of surface phonons in pure graphite. The different modes are the vertical acoustical mode ZA, the acoustical shear horizontal mode SH, the longitudinal acoustical mode LA, the vertical optical mode ZO, the optical shear horizontal mode SH*, and the longitudinal optical mode LO. Triangles depict the data for θ_i=60°, circles for θ_i=70°, and squares for θ_i=75°. Open symbols denote peaks with poor signal-to-noise ratio. The lines represent a mere guide to the eye.

published only for the ΓM direction. In the following we will present our own calculations following this model.

B. Pure graphite: Calculations

The model by Aizawa *et al.* was derived to describe the phonons in MLG's on carbides. Due to the weak interaction between the single graphite layers it describes the (surface) phonons of pure graphite as well.[13] The interactions and force constants taken into account are summarized in Table I. The interaction potentials as described in Ref. 13 were used to determine the dynamical matrix and from its eigenvalues the phonon dispersion. The polarization of the individual modes follows from the corresponding eigenvectors of the dynamical matrix. As a first approach we used the force constants found for graphite in the ΓM direction[13] and calculated the dispersion along ΓK. The result is seen in Fig. 4 (dotted lines) together with our experimental dispersion. The agreement is already quite good; however, the SH, LA, and ZO modes are overestimated for the most part of the Brillouin zone. Therefore we tried to find a new set of parameters that better describes the data. Although we did not use a least-squares procedure to fit the parameters the new set reproduces the data better, as seen by the solid lines in Fig. 4. A comparison between the force constants used by Aizawa *et al.* and our new force constants is given in Table II. The fit for the dispersion in the K direction requires slightly lower stretching and out-of-plane bending force constants whereas

TABLE I. Interactions and force constants of the model by Aizawa *et al.* For details of the interactions and the potentials refer to Aizawa *et al.* (Ref. 13).

Type of interaction	Force constant
Nearest-neighbor stretch	α_1
Second-nearest-neighbor stretch	α_2
In-plane bend	γ_1
Out-of-plane bend	γ_2
Twist	δ
Vertical interaction with substrate	α_s

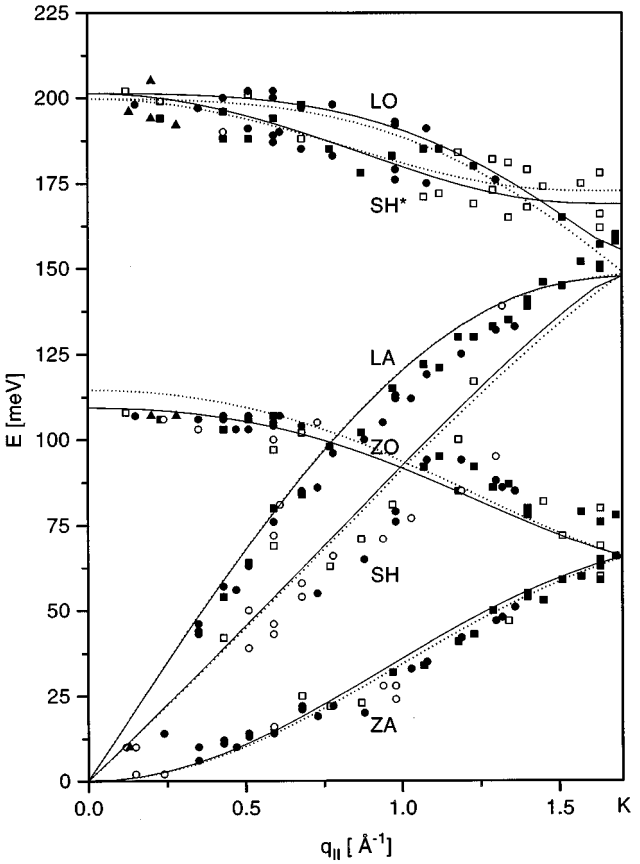

FIG. 4. The dispersion relation of the surface phonons in pure graphite calculated according to the model by Aizawa *et al.* using the parameters derived for the dispersion along ΓM (dotted line) and using parameters newly ''fitted'' for the dispersion along ΓK (solid line) together with our experimental results.

the in-plane bending and the twisting force constant turned out somewhat higher. The lattice constant is not a parameter in the case of pure graphite. Of course there needs to be a single set of parameters for both directions eventually.

An open fundamental problem is the splitting of the ZA and the ZO mode at the *K* point. The frequencies at the *K* point as derived from the model by Aizawa *et al.* are the following:

TABLE II. Actual values of force constants for pure graphite used by Aizawa *et al.* (Ref. 13) in comparison with our set of parameters (a_0 in our case represents the equilibrium nearest-neighbor distance whereas in the Aizawa paper a represents the lattice constant $a=\sqrt{3}a_0$; a or a_0 is not a fit parameter for pure graphite).

		Our value	
Parameter	Aizawa's value	For graphite	For GIC
a_0 (Å)	1.42	1.42	1.42
α_1 (N/m)	364	344	285
α_2 (N/m)	62	62	100
γ_1 $(10^{-19}$ J)	8.30	9.3	7.6
γ_2 $(10^{-19}$ J)	3.38	3.08	2.2
δ $(10^{-19}$ J)	3.17	4.17	7.5
α_s (N/m)	0	0	8.5

$$\omega_{1,2}=\left[\frac{1}{m}\left(2\alpha_s+\frac{3\delta}{a_0^2}+\frac{9\gamma_2}{a_0^2}\right)\right]^{1/2},$$

$$\omega_3=\left[\frac{1}{2m}\left(9\alpha_2+\frac{36\gamma_1}{a_0^2}\right)\right]^{1/2},$$

$$\omega_{4,5}=\left[\frac{1}{2m}\left(3\alpha_1+9\alpha_2+\frac{9\gamma_1}{a_0^2}\right)\right]^{1/2},$$

$$\omega_6=\left(\frac{1}{2m}(6\alpha_1+9\alpha_2)\right)^{1/2},$$

where m is the mass of the C atoms and the other parameters are described in Tables I and II.

The model by Aizawa *et al.* requires ZA and ZO ($\omega_{1,2}$) to be degenerate, but the experimental evidence is clearly in favor of the splitting. The other theoretical approaches known to us[19–21] also show a degeneracy of the ZA and the ZO mode at the *K* point.

The model by Aizawa *et al.* also requires two of the four higher frequencies to be degenerate. From our experimental data these seem to be the LO and LA mode but as seen from Fig. 3 the experimental base is weak. It is possible to find a set of parameters that results in the degeneracy of these two modes at the *K* point. But then the dispersion relation of LA is not well described for most of the Brillouin zone. We therefore decided to choose a set of parameters that describes the behavior within most of the Brillouin zone reasonably well although the degeneracy at the *K* point might not be given properly.

C. Lanthanum carbide

Upon evaporation of a rather thick La film and annealing to 1000 K a surface layer of lanthanum carbide of unknown stoichiometry is formed,[5] indicated in LEED by a $\sqrt{3}$-like superstructure[6] and in AES by the typical triplet structure.[5] In our experiment the LEED pattern was clarified to be a $(1\times2\sqrt{3})$ structure and the AES showed clearly the typical carbide structure. For this phase we measured the surface vibrations as well. Here we do not expect the surface phonons to correlate closely to the bulk phonons as they do in graphite. To our knowledge no data exist for either the bulk or the surface phonons of any modification of lanthanum carbide. The closest information available is the dispersion of the bulk phonons of TaC and HfC.[22] Both materials show strongly dispersing phonon modes with energies up to 90 meV. Our results for the surface phonons are shown in Fig. 5. Five dispersionless features can be distinguished at 43, 63, 104, 121, and 205 meV. The HREEL spectra usually show a rather broad peak around 205 meV, making it difficult to determine the exact peak position; thus energy values for this mode scatter a lot.

It is known for other semiconductors as well that the surface phonons show very little dispersion[23] whereas the bulk phonons are strongly dispersing. However, the surface phonons are not higher in energy than the bulk phonons. So if we assume that the bulk phonons of our lanthanum carbide here are similar to those in TaC and HfC with maximum energies around 100 meV the modes in Fig. 5 cannot all represent surface phonons of the La carbide.

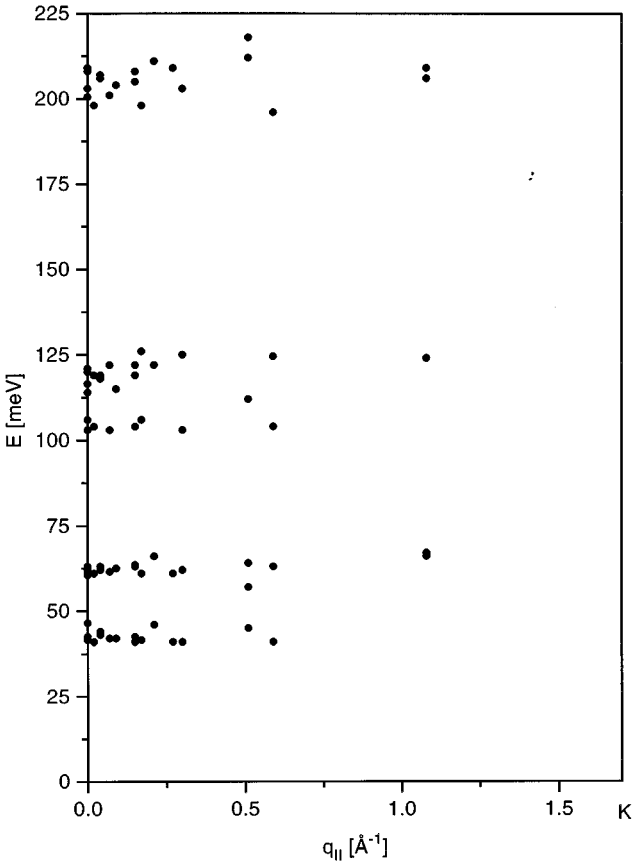

FIG. 5. Vibrations of the carbidic phase as measured with HREELS.

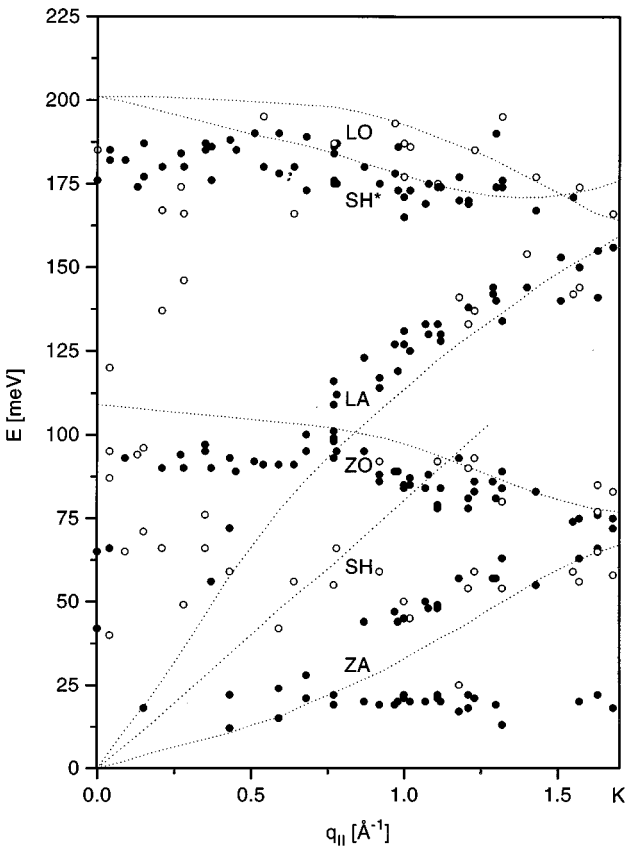

FIG. 6. The dispersion relation of the GIC-like layer on lanthanum carbide, annealed at 1500 K, as determined by HREELS in comparison with the one of pure graphite (dotted lines, taken from the guide to the eye from Fig. 3). The same modes as in graphite are observed with characteristic energy shifts plus an additional low-energy mode. Open circles denote again loss peaks with poor signal-to-noise ratio.

A more natural explanation is the starting formation of a graphitic layer forming islands on top of the carbide—thus what we see here are the Einstein modes of these islands corresponding to graphite phonons in high symmetry points. The mode at 205 meV agrees with the LO mode at the Γ point, the 104-meV one to the ZO at Γ, the 63-meV one to the ZA at K, the one at 121 meV might correspond to the SH mode at K. The origin of the 43-meV mode is unclear at the moment; it might still be a surface mode of the carbide.

D. La-GIC-like layer: Experiment and calculations

With further annealing of the system to 1300 K or higher temperatures a GIC-like layer—either a monolayer of graphene (MLG) or a thin layer of a graphite intercalated compound—forms on top of the lanthanum carbide,[6] which manifests itself in the LEED pattern as a clear $(\sqrt{3}\times\sqrt{3})R30°$ structure and in an electronic structure very much like that of alkali metal GIC's (Ref. 5) indicating charge transfer from the metal atoms in the carbide or the GIC to the carbon atoms in the graphene layer. In our experiment we saw the clear LEED pattern as well as a clear peak at 280 eV in the Auger spectrum indicating the same geometrical and electronic structure as in the previous experiments. Both results—the LEED pattern and the 280-eV Auger peak—are fully observed already at annealing temperatures of 1300 K and do not change upon annealing to 1500 K.

The surface-phonon dispersion for the GIC-like layer annealed at 1500 K is very similar again to the one observed in graphite as seen in Fig. 6. The scatter of the data is much higher than in graphite. This might be due to some inhomogeneties throughout the sample. Still the same six modes are detected although the shear horizontal mode is not seen in most spectra as expected from the HREELS selection rules. An additional mode is observed at low energies plus some additional data points that do not agree with any of the modes—these will be discussed below. Compared to the modes in graphite the modes of the GIC-like layer are shifted in energy. The three optical modes soften whereas the LA and ZA modes stiffen, the SH mode is hardly detected. This is unlike the behavior observed in MLG on transition-metal carbides: there all modes soften.[12,13]

Still the model by Aizawa *et al.* can be used to describe the observed modes as seen by the solid lines in Fig. 7(a). The agreement for all the modes is within the experimental error besides for the hardly detected SH mode and the splitting of ZO and ZA modes at the K point. The force constants used are shown in Table II. The splitting of ZO/ZA could have been described by using a larger Brillouin zone and thus a smaller nearest-neighbor distance a_0. But since the splitting already occurs in graphite and since the overall fit with the smaller a_0 was not better than the one shown here we decided to maintain the graphite lattice constant. The nearest-neighbor stretching force constant is lower for the

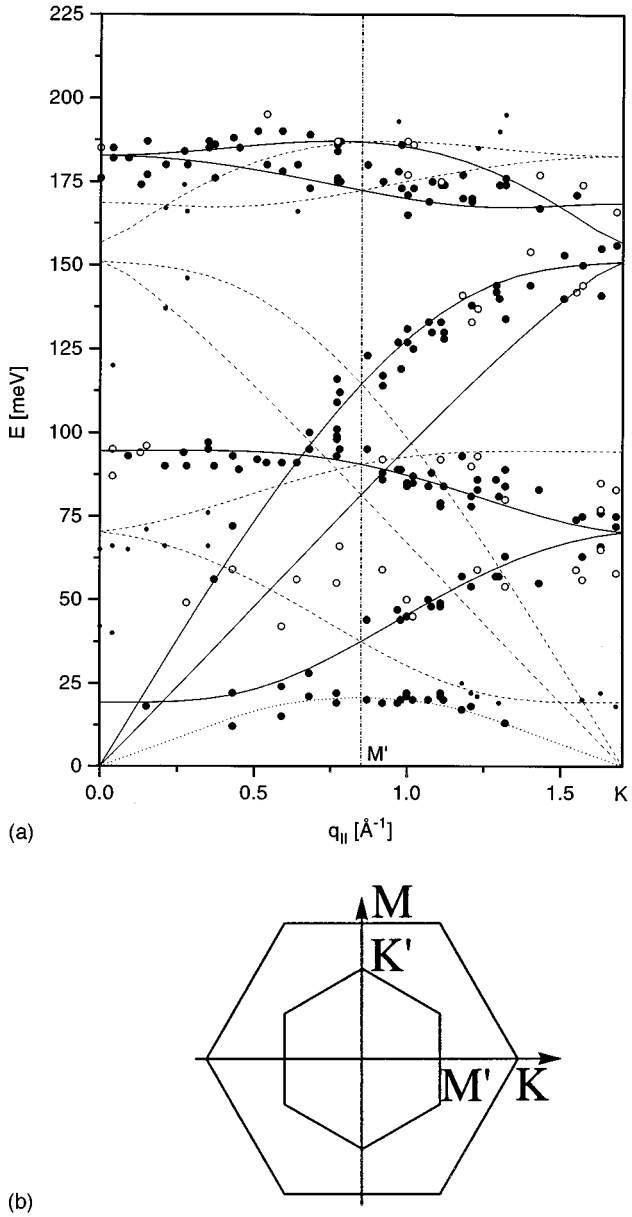

FIG. 7. (a) The same dispersion relation as in Fig. 6 together with the one calculated according to the model by Aizawa *et al.* (solid lines). The calculated dispersion relations folded according to the $(\sqrt{3}\times\sqrt{3})R30°$ superstructure are shown as dashed lines. Small circles denote data points belonging to folded modes. The dotted line represents a guide to the eye for the low energy mode. (b) The relation between the Brillouin zone for graphite and for a $(\sqrt{3}\times\sqrt{3})R30°$ superstructure.

GIC-like layer than for graphite as one might expect from the softening of the optical modes. In contrary the second-nearest-neighbor stretching force constant is considerably higher to account for the stiffening of the acoustical modes. The in-plane and out-of-plane bending force constants are lower than for graphite, whereas the twisting force constant is much higher for the GIC-like layer. This is in accord with the behavior of the stretching force constants since the bending can be considered a mostly nearest-neighbor interaction whereas the twisting includes further neighbors as well. The cause of this behavior is discussed in the following.

For the GIC-like layer the ZA mode shows an energy gap at the Γ point. This is taken into account by including the vertical interaction with the substrate, i.e., $\alpha_s \neq 0$ (cf. Table II). In pure graphite α_s equals zero due to the weak van der Waals interaction between the layers. The energy gap of the ZA mode is also observed in MLG on transition-metal carbides. There the strong interaction is due to covalent bonds between the carbon atoms in the MLG and the metal atoms of the carbide[14,16] resulting in a higher energy gap of 35 meV compared to 20 meV here. In our case the interaction between the GIC-like layer and the substrate must be caused by the charge transfer observed in the AES. The transferred charge occupies the antibonding π^* bands in the graphene, thus weakening the π bonds and reducing the nearest-neighbor coupling constants. Why the second-nearest-neighbor coupling constants increase is not clear at the moment. Calculations using the bond charge model[21] might help since they explicitly include the bond electrons.

In our LEED investigation we have observed a $(\sqrt{3}\times\sqrt{3})R30°$ superstructure. Therefore one expects a smaller Brillouin zone to be reflected in the phonon dispersion. The Brillouin zone corresponding to the $(\sqrt{3}\times\sqrt{3})R30°$ superstructure is shown in Fig. 7(b). The M' point of the new Brillouin zone is located halfway between Γ and K of the graphite Brillouin zone as indicated by the dash-dotted line in Fig. 7(a). The phonon modes should fold at this line resulting in the dashed lines in addition to the solid lines. As seen from this lines most of the previously unaccounted for points can be considered as representing folded modes. The $(\sqrt{3}\times\sqrt{3})R30°$ superstructure is caused by the structure of the La atoms (of the carbide or intercalated between two graphite layers) underneath every other graphene hexagon. Any phonons within this La layer would be expected to show clearly the folding at the Brillouin zone boundary at M'. Furthermore they should appear at lower energies than the graphite phonons due to the much higher mass of the La atoms. This is most likely what we see in the low-energy mode represented in Fig. 7(a) by the dotted line.

In Fig. 8 we show the dispersion relation of the GIC-like layer annealed at 1300 K as well (diamonds). It shows the same modes as the system annealed at 1500 K with comparable energies for the LO, SH*, and ZO modes. However, the LA and ZA modes agree much better with the modes of pure graphite. The SH mode is hardly detected. This is the first hint of an additional phase at high annealing temperatures. No traces of the graphite dispersion relation are seen in the carbide phase. So it seems that an MLG forms at annealing temperatures of 1300 K on top of the carbide. The layered structure is then of the form (from top) C(graphene)-LaC_2(La terminated). The charge transfer is already complete in this phase as indicated in the AES by 280-eV peaks of the same intensity for annealing at 1300 K or at 1500 K. But annealing at 1500 K still changes the dispersion relation of the LA and the ZA mode from graphite-like to higher energies. One possible reason for this behavior is the restructuring of the second layer underneath the LaC_2 surface, which consist of C atoms[6] to form another graphene layer thus forming a GIC of the structure: C(graphite)-La(intercalated)-C(graphite)-LaC_2(C terminated). Another explanation for this two-phase behavior could be a change of yet unknown nature of the MLG itself.

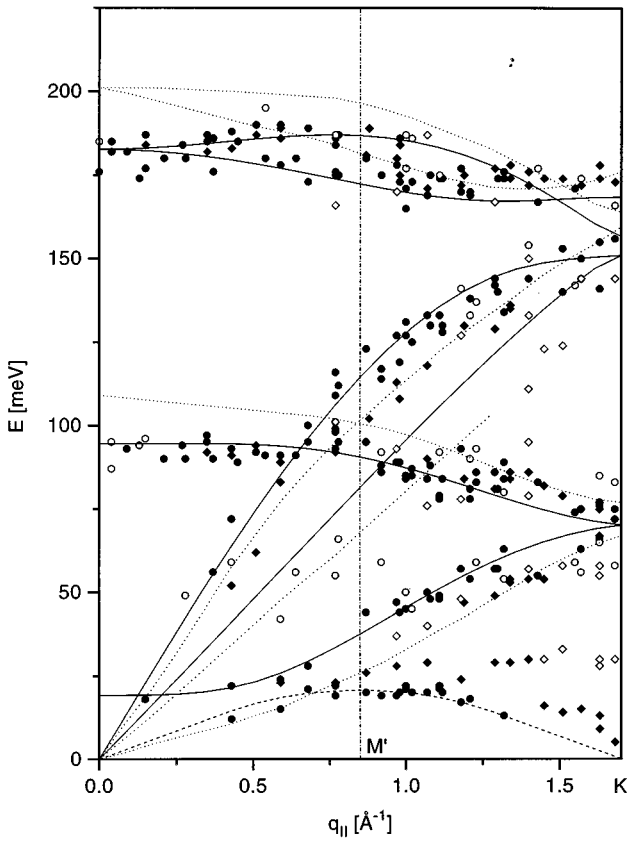

FIG. 8. Comparison of the phonon dispersion of the GIC-like layer annealed at 1500 K (circles) to the one obtained after annealing to 1300 K (diamonds). The dotted lines show again the graphite dispersion relations, the solid lines the calculated phonons for the 1500 K phase, and the dashed line the mode within the La layer. Open symbols denote again peaks with poor signal-to-noise ratio.

Comparison of our dispersion relations to the phonons observed in other GIC's does not help to answer the question since hardly any information is available on the in-plane propagating phonons in GIC's. The optical modes soften[17] as they do here or in MLG's on carbides. And it is known for Li-GIC that the ZA mode softens[18] as in MLG but unlike in the La-C system here. So the two-phase model with a transition from MLG to GIC seems to us the most natural explanation.

There are a few data points at low energy and high momentum transfer that are not accounted for by either the GIC type or the graphite type dispersion relations. They could be a hint of folded graphite type SH and LA modes. This assumption gives a description satisfactory within the experimental error for all these additional points except the three at highest momentum transfer around 20 meV. These must remain open for the time being. Since the $(\sqrt{3}\times\sqrt{3})$ structure is already clearly present at 1300 K annealing temperature one would expect to see at least traces of folded bands for this phase—as we do.

IV. CONCLUSION

The phonon dispersion relations of graphite have been measured in the ΓK direction over the whole energy range. They have been described within the model by Aizawa *et al.* One feature that has not been accounted for yet in all the models known to us is the splitting of the ZA and ZO mode at the K point.

Following the procedure used before in electronic structure studies of the La-graphite system we first investigated the vibrations in the carbidic phase and then those of the GIC-like phase. The superstructure of the carbidic phase is now clarified to be a $(1\times2\sqrt{3})$ structure. The energy-loss peaks in this phase show no dispersion and represent most likely the Einstein modes of graphite islands growing on top of the carbide.

The GIC-like phase shows again the six phonon modes observed in graphite with the optical modes shifted towards lower energies whereas the acoustical phonons are shifted to higher energies. This can be accounted for within the model by Aizawa *et al.* by weaker nearest-neighbor interactions and stronger second-nearest-neighbor interactions. The nearest-neighbor bonds are weakened by a charge transfer from the La atoms to the graphite layer that occupies the antibonding π^* bands, as seen in the Auger spectra. The source of strengthening of the second-nearest-neighbor bond is not clear at the moment.

A folding of the phonon modes due to the $(\sqrt{3}\times\sqrt{3})$ superstructure as seen in LEED is weakly observed. An additional low-energy mode is attributed to a phonon in the La layer.

At an annealing temperature lower than that of the final GIC-like phase an additional phase is observed characterized by the same softening of the optical modes as in the GIC-like phase and unchanged acoustical modes. This is an experimental hint that the final phase represents a thin GIC layer and not a mere monolayer of graphene.

ACKNOWLEDGMENTS

This work was supported by the Deutsche Forschungsgemeinschaft, by the program ''Fullerens and atomic clusters,'' by the Russian Fund of Fundamental Investigation, and by the exchange program between the Free University Berlin and the St. Petersburg State University. A.M.Sh is grateful to Free University Berlin for financial support and hospitality. S. S. acknowledges financial support by the Hochschulsonderprogramm II of the Free University. We all are indebted to Dr. Weiβ of Graphitwerk Kropfmühl AG, Munich, and Dr. Molodtsov of Technical University Dresden for providing us with the very big graphite flakes.

*Present address: Hahn-Meitner-Institut, Glienicker Str. 100, D-14109 Berlin, Germany.

[1] A. M. Shikin, G. V. Prudnikova, A. V. Fedorov, and V. K. Adamchuk, Surf. Sci. **307–309**, 205 (1994).

[2] C. Oshima, T. Aizawa, R. Souda, Y. Ishizawa, and Y. Sumiyoshi, Solid State Commun. **65**, 1601 (1988).

[3] J. L. Wilkes, R. E. Palmer, and R. F. Willis, J. Electron Spectrosc. Relat. Phenom. **44**, 355 (1987).

[4] G. V. Prudnikova, A. G. Vjatkin, A. V. Ermakov, A. M. Shikin, and V. K. Adamchuk, J. Electron Spectrosc. Relat. Phenom. **68**, 427 (1994).

[5] A. M. Shikin, S. L. Molodtsov, C. Laubschat, G. Kaindl, G. V.

Prudnikova, and V. K. Adamchuk, Phys. Rev. B **51**, 13 586 (1995).
[6] A. Vyatkin, S. Gorovikov, A. Shikin, V. Adamchuk, J. Avila, M.-C. Asensio, and S. L. Molodtsov, Phys. Low-Dimen. Struct. **12**, 339 (1995).
[7] S. L. Molodtsov, Th. Gantz, C. Laubschat, A. G. Viatkine, J. Avila, C. Casado, and M. C. Asensio, Z. Phys. B **100**, 381 (1996).
[8] S. L. Molodtsov, C. Laubschat, M. Richter, Th. Gantz, and A. M. Shikin, Phys. Rev. B **53**, 53 (1996).
[9] S. A. Gorovikov, A. M. Shikin, G. V. Prudnikova, A. G. Vjatkin, and V. K. Adamchuk, Phys. Low-Dimen. Struct. **10/11**, 29 (1995).
[10] M. E. Makrini, D. Guérard, P. Lagrange, A. Herold, Physica B **99**, 481 (1980).
[11] R. Kaplan, Surf. Sci. **215**, 111 (1989); L. Li and I. S. T. Tsong, Surf. Sci. **351**, 141 (1996); R. Gunnella, J. Y. Veuillen, A. Berthet, and T. A. Nguyen Tan, Surf. Rev. Lett. (to be published).
[12] T. Aizawa, R. Souda, S. Otani, Y. Ishizawa, and C. Oshima, Phys. Rev. Lett. **64**, 768 (1990).
[13] T. Aizawa, R. Souda, S. Otani, Y. Ishizawa, and C. Oshima, Phys. Rev. B **42**, 11 469 (1990); **43**, 12 060 (E) (1991).
[14] A. Nagashima, K. Nuka, K. Satoh, H. Itoh, T. Ichinokawa, C. Oshima, and S. Otani, Surf. Sci. **287/288** 609 (1993).
[15] A. Nagashima, H. Itoh, T. Ichinokawa, and C. Oshima, Phys. Rev. B **50**, 4756 (1994).
[16] K. Kobayashi and M. Tsukuda, Phys. Rev. B **49**, 7660 (1994).
[17] M. S. Dresselhaus and G. Dresselhaus, Adv. Phys. **30**, 139 (1981), and references therein.
[18] A. Magerl, H. Zabel, and J. J. Rush, Synth. Met. **7**, 339 (1983).
[19] G. Kresse, J. Furthmüller, and J. Hafner, Europhys. Lett. **32**, 729 (1995).
[20] P. Pavone (private communication); for the approach see P. Giannozzi, S. de Gironcoli, P. Pavone, and S. Baroni, Phys. Rev. B **43**, 7231 (1991).
[21] G. Benedek and G. Onida, Phys. Rev. B **47**, 16 471 (1993).
[22] H. Bilz and W. Kress, *Phonon Dispersion Relations in Insulators* (Springer, Berlin, 1979).
[23] H. Nienhaus, *Festkörperprobleme: Advances in Solid State Physics* (Vieweg, Braunschweig, in press), Vol. 36.